IMECE2017-70220

BLADELETS – WINGLETS ON BLADES OF WIND TURBINES:

A MULTIOBJECTIVE DESIGN OPTIMIZATION STUDY

Sohail R. Reddy
Florida International University
Department of Mechanical and Materials Eng.
MAIDROC Laboratory, Miami, FL 33174, USA.
sredd001@fiu.edu

George S. Dulikravich
Florida International University
Department of Mechanical and Materials Eng.
MAIDROC Laboratory, Miami, FL 33174, USA.
dulikrav@fiu.edu

Helmut Sobieczky
Vienna University of Technology
Institute of Fluid Mechanics and
Heat Transfer, 1010 Vienna, Austria
helmut@sobieczky.at

ABSTRACT

The work presented in this paper used rigorous 3D flow-field analysis combined with multi-objective constrained shape design optimization for the design of complete blade + bladelet configurations for a three-blade propeller type wind turbine.

The fluid flow analysis in this work was performed using OpenFOAM software. The 3D, steady, incompressible, turbulent flow Reynolds-Averaged Navier-Stokes equations were solved in the rotating frame of reference for each combination of wind turbine blade and bladelet geometry. The free stream uniform wind speed in all cases was assumed to be 9 m s^{-1}.

The three simultaneous design optimization objectives were: a) maximize the coefficient of power, b) minimize the sensitivity of the design to minor geometric perturbations, and c) minimize twisting moment around the blade axis. The bladelet geometry was fully defined by using a small number of parameters. The optimization was carried out by creating a multi-dimensional response surface for each of the simultaneous objectives.

The response surfaces were based on radial basis functions, where the support points were designs analyzed using the high fidelity CFD analysis of the full blade + bladelet geometry. The response surfaces were then coupled to an optimization algorithm in modeFRONTIER software. The predicted values of the objective functions for the optimum designs were then again validated using OpenFOAM high fidelity analysis code.

---

*   Ph.D. Student Presidential Fellow. Student Member ASME.
**   Director of MAIDROC Laboratory. Fellow ASME.
*** Professor.

Results for a Pareto optimized bladelet on a given blade indicate that more than 9% increase in the coefficient of power at minimal thrust force penalty is possible compared to the same wind turbine rotor blade without a bladelet.

1. INTRODUCTION

Although much work has been reported on design of winglets on airplane wings [1,2], the volume of published efforts to design bladelets (winglets at the tips of the wind turbine blades) for rotating lifting surfaces is still very limited. This is especially true for mathematical optimization of bladelets for propeller type wind turbine blades.

In recent years, a strong push towards energy independence and clean, renewable energy has resulted in significant advances in the area of solar, wind and nuclear energy. In 2015, 11% of energy produced was renewable energy, 19% of which was harvested from the wind. Bazmi and Zahedi [3] stated that wind power is the second fastest growing renewable energy with an annual growth rate of 34%. Evans *et al.* [4] showed that wind power led to lowest greenhouse gas emission, least water consumption and most favorable social impact than geothermal, hydropower and solar energy.

For large scale applications, such as offshore wind farms, horizontal axis wind turbines (HAWT) are the preferred choice. Although the wind turbines have become more efficient over the decade, their basic shape has remained unaltered.

Winglets have previously been investigated for their ability to increase the efficiency of the propeller type wind turbines.

Wind turbines have previously been extensively studied. Zhao *et al.* [5] performed computational aerodynamic analysis on upwind and downwind turbine configurations. Wood and Deiterding [6] used a detailed Lattice Boltzmann method to perform a fully 3D turbulent flow analysis of HAWT configurations. Tobin *et al.* [7] experimentally investigated the effects on winglets on wake and performance of wind turbines. Their work showed an increase in power and thrust coefficients by 8% and 15%, respectively. Gaunaa and Johansen [8] numerically investigated the aerodynamic efficiency of turbine rotors with winglets. They reported the increase in power is due to the reduction of tip losses and is not connected with a downwind shift of wake vorticity. Gertz *et al.* [9] experimentally investigated the effects of wind speeds and rotor rotation speeds on power production. Ferrer and Munduate [10] used CFD analysis to carry out a blade tip comparison study. To the authors' knowledge, never before has a multi-objective optimization study of the bladelet configuration been published.

2. ANALYSIS

2.1 Geometry Definition

The standard Vestas27 wind turbine blade geometry [11] of a 13.5 m radius rotor was used as the benchmark in this work. This blade geometry was not changed for any CFD analysis performed in this work.

Different bladelets were virtually added to the tip of the Vestas27 blade. Only bladelet shapes were optimized, while the blade geometry was kept unchanged.

When performing shape optimization in any discipline, an efficient manner for representing geometry is needed in order to minimize the number of variables that the optimization algorithm will have to use. Defining the geometry with an inadequate number of parameters leads to a restricted design space for the multi-objective optimizer. Conversely, defining the geometry with excessive number of design variables leads to an over sensitive design and often wastes computational resources.
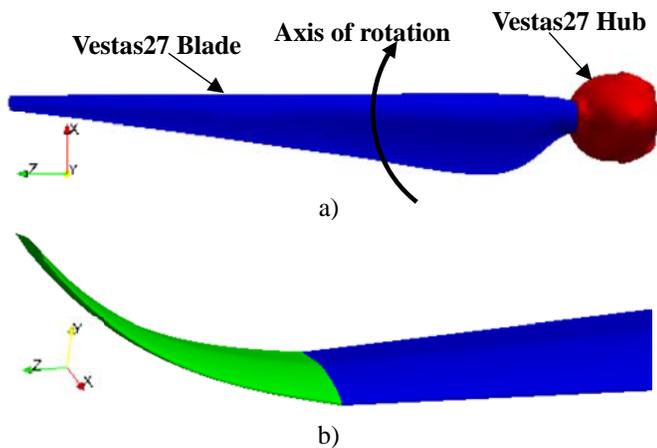

a)

b)

Figure 1. Geometry for a) baseline Vestas27 wind turbine blade, and b) retrofitted with a bladelet at the tip of the Vestas27 blade.

Each bladelet configuration in this study was defined using five variables: bladelet span, twist angle, dihedral angle, sweep angle, and taper ratio. Figure 1 show the Vestas27 blade used in this study and a typical bladelet configuration. Details of the Vestas27 geometry are given in Ref. [11]. The dihedral angle was defined as a second order polynomial to satisfy continuity conditions at the bladelet root and blade tip. All other parameters were chosen to vary linearly as a function of bladelet span. The approximate range for each parameter is shown in Table 1.

Table 1. Allowable range and step size for each geometric design variable used to define the bladelet configurations

	Min.	Max.	Step Size
Span (m)	0.1	1.5	0.1
Twist Angle (degrees)	-20.0	20.0	1.0
Dihedral Angle (degrees)	-45.0	45.0	1.0
Sweep Angle (degrees)	-45.0	45.0	1.0
Taper Ratio	0.1	1.0	0.1

2.2 Computational Method

The computational grid of hexahedral cells for each candidate blade+bladelet configuration was generated using cfMesh [12]. A total of 10 layers of grid cells were placed within the viscous sublayer. Figure 2 shows the relative dimensions of the computational domain where R is the rotor radius. Only 1/3 of the entire wind turbine configuration was analyzed due to the periodicity of the geometry. Each configuration was analyzed for the uniform axial free stream air speed of 9 m s^{-1} with the rotor rotating at 12 rpm.
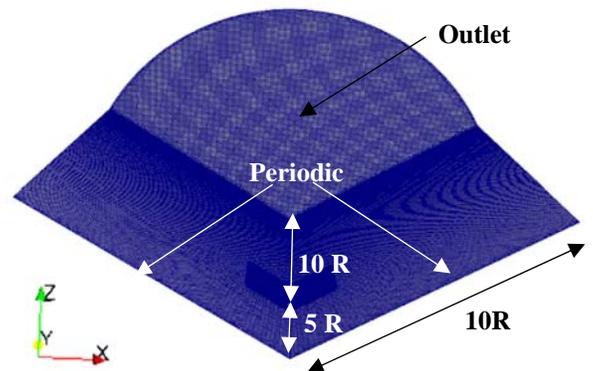

Figure 2. Dimensions of the computational domain used to analyze each blade+bladelet geometry.

The optimization objective function values for each blade+bladelet configuration were obtained by performing a full 3D, turbulent fluid flow analysis in OpenFOAM software [13]. The built-in solver MRFSimpleFoam was used to simulate the wind turbine configuration in a rotating frame of reference. The mass and momentum conservation equations for incompressible viscous flow were solved using finite volume method.

$$\nabla \cdot \vec{V}_a = 0 \qquad (1)$$

$$\nabla \cdot \vec{V}_r = -\frac{\nabla p}{\rho} + (\mu_\ell + \mu_t)\nabla^2 \vec{V}_a - \vec{\Omega} \times \left(2\vec{V}_r - \vec{\Omega} \times \vec{r}\right) \quad (2)$$

$$\vec{V}_a = \vec{V}_r + \vec{\Omega} \times \vec{r} \qquad (3)$$

Here, $\vec{\Omega}$ is the steady angular velocity of the wind turbine rotor, μ_ℓ and μ_t are dynamic viscosity coefficients for laminar and turbulent flow, $\vec{V}_r$ is velocity relative to the blade, $\vec{V}_a$ is absolute velocity, $\vec{r}$ is position vector in the rotor plane, ρ is density of air, and p is local pressure.

The utilized flow-field analysis software OpenFOAM was validated on the benchmark NREL 5-MW baseline wind turbine by Zhao *et al.* [14,15]. The κ-ω-SST turbulence model proposed by Menter [16] was employed to model turbulence. The κ-ω-SST was extensively utilized in the simulation of wind turbine aerodynamics with results being in good agreement with experiments [14,15].

2.3 Optimization Procedure

It should be pointed out that this study did not involve shape optimization of the blade. An unchanged shape of the rotor blade was used together with the bladelet when optimizing the bladelet shape and size. This study did not involve simultaneous shape optimization of both blade and the bladelet. The multi-objective optimization of the bladelet configuration was carried out using the commercial software package modeFRONTIER [17]. The five parameters in Table 1 are selected as the design parameters that need to be optimized. The three simultaneous objectives are to maximize the coefficient of power and minimize the coefficient of twisting moment and thrust coefficient. The coefficients of power is defined as [18]

$$C_P = \frac{P}{\rho V_\infty^3 A} \qquad (4)$$

The coefficient of axial thrust force is defined as [18]

$$C_T = \frac{T}{\rho V_\infty^2 A} \qquad (5)$$

Here, P is the power output and T is the axial thrust force. The power output by the wind turbine is calculated as

$$P = M\Omega \qquad (6)$$

where M is the torque around the rotor axis generated by the rotor and Ω is the angular speed of the rotor.

Because the computational time for each analysis is so large, an alternative, much faster method is required to compute the objective functions. For this reason, surrogate models were used to obtain the objective function values for each blade+bladelet configuration. A response surface based on Hardy's multiquadrics radial basis functions [19] was created for each of the three objectives. It is well known that the accuracy of the response surface is greatly influenced by the distribution of the support points used to construct it. Consequently, an initial population of 50 candidate designs were created using SOBOL's [20] pseudo-random number generator that uniformly distributed the candidate designs within the five-dimensional design space. All three response surfaces were then coupled to the NSGA-II [21] multi-objective optimization algorithm to search the design and objective function space for Pareto optimal designs. The maximum allowable coefficient of power was limited to the Betz Limit of 0.592 to limit search to the feasible domain. Figure 3 shows the optimization methodology implemented in this work.
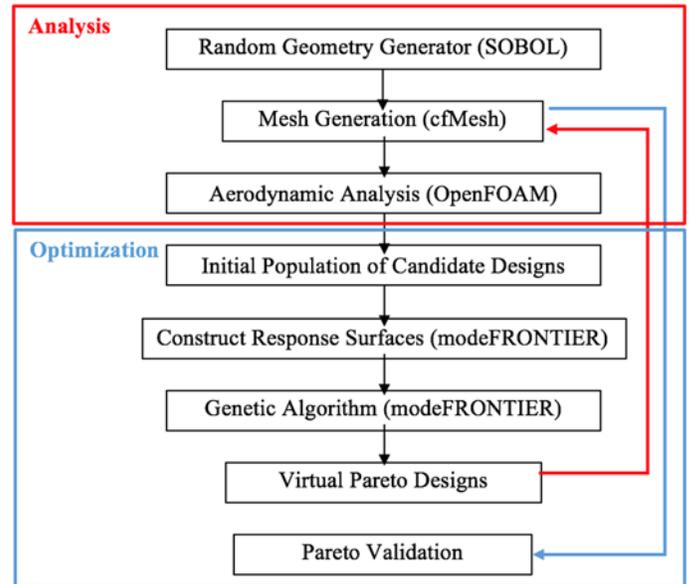

Figure 3. Workflow of the optimization framework.

3. AERODYNAMIC ANALYSIS

3.1 Aerodynamic Analysis of VESTAS27 Blade

As the performance benefits of various bladelet configurations are being analyzed, a benchmark case is needed for comparison. For this reason, the Vestas27 blade aerodynamic performance was analyzed using OpenFOAM software at a freestream velocity of 9 m s^{-1} rotating at 12 rpm. The velocity of the blade and pressure on the surface of the blade are shown in Fig. 4. It can be seen from Fig 4a, that the velocity computed at the blade tip using Eq. (3) for a rotor radius of the Vestas27 blade (13.5m) matched as expected with the blade tip velocity obtained from OpenFOAM software. The values of the three coefficients (objective functions) for this benchmark are given in Table 2.
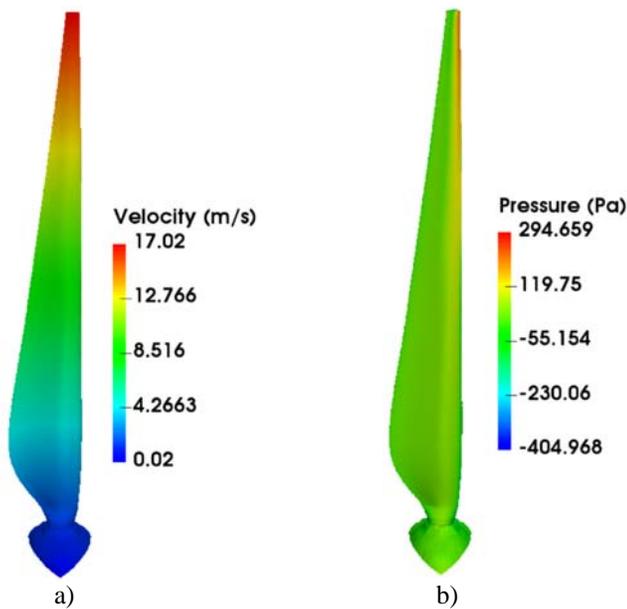
Figure 4. a) Relative velocity, and b) pressure field on the surface of the Vestas27 blade

Table 2. Objective function values for the benchmark Vestas27 blade without a bladelet (C_M is aerodynamic twisting moment)

C_P	C_T	C_M
0.083	0.075	0.040

4. OPTIMIZATION RESULTS

Due to conflicting objectives, the multi-objective optimization algorithm arrives at a Pareto frontier of best trade-off solutions rather than a single global optimum. Figure 5 shows the Pareto frontiers arrived at using the NSGA-II algorithm.
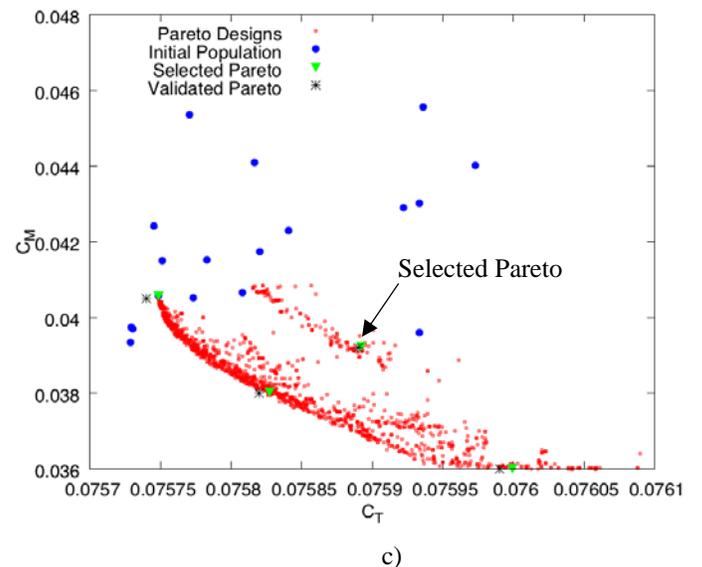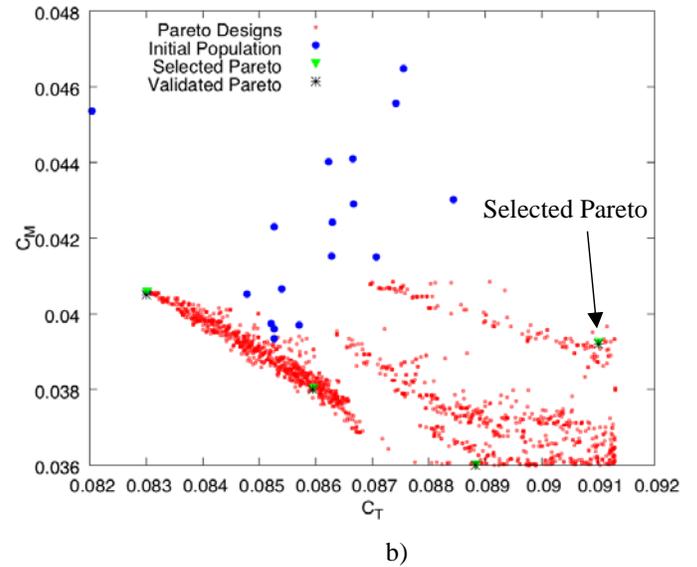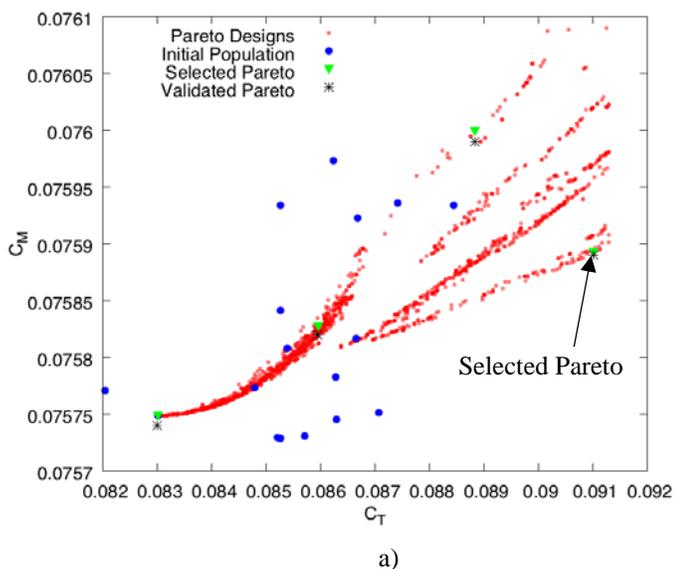

a)

b)

c)

Figure 5. Response surface points for a) C_P *vs.* C_T, b) C_P *vs.* C_M and c) C_T *vs.* C_M

Because the accuracy of the response surface deteriorates in regions within and outside the design space, four virtual bladelet configurations were selected at random from the Pareto frontier and analyzed using OpenFOAM. The objective function values obtained from the response surface deviated by 3% from the ones obtained from CFD analysis. The five design parameters of the four virtual Pareto optimized designs were than randomly perturbed by 2% to simulate defects due to manufacturing tolerance in an effort to study the sensitivity of the designs. The design parameters of the least sensitive wind turbine blade+optimized bladelet are given in Table 3. Figure 6 shows the velocity and pressure field on the surface of the unoptimized blade and the optimized bladelet.

Table 3. Pareto optimized values of the five design variables and objective functions of the Pareto optimized configuration

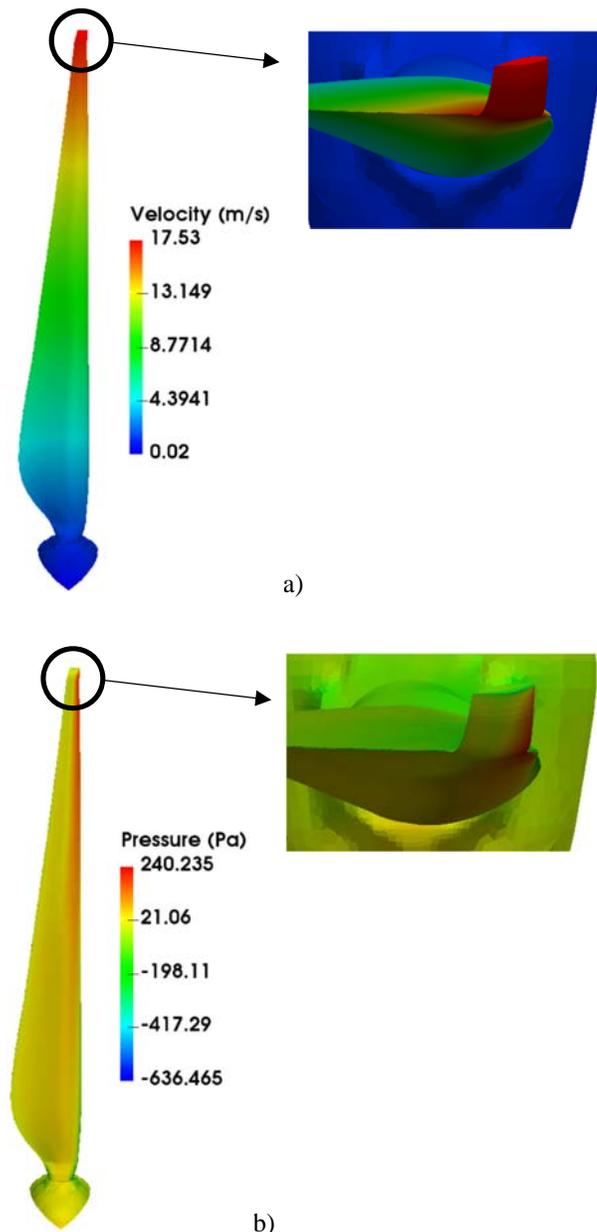|	
Span (m)	0.4
Twist Angle	-17.0
Dihedral Angle	6.0
Sweep Angle	-16.0
Taper Ratio	0.7
C_P, ΔC_P %	0.0910, +9.6
C_T, ΔC_T %	0.0759, +1.3
C_M, ΔC_M %	0.0394, -2.5

a)

b)

Figure 6. a) Relative velocity, and b) pressure field on the surface of the unoptimized blade + optimized bladelet configuration.

From the initial population of 50 candidate blade+bladelet shapes, the NSGA-II optimization algorithm was able to find other wind turbine bladelet designs that perform better than the initial population. The range of increase in coefficient of pressure due to the addition of optimized bladelets is in good agreement with the results presented in other studies. [8,9]. The addition of optimized bladelet resulted in a 9.6% increase in C_P and 2.5% decrease in the blade twisting moment, while increasing the coefficient of axial thrust force by 1.3%.

CONCLUSION

This work investigated the effectiveness of bladelets on the tips of wind turbines on increasing wind turbine rotor power output. Each blade+bladelet configuration was analyzed using the OpenFOAM solver MRFSimpleFoam. Multi-objective optimization was performed on the bladelet configuration only (not on the blade configuration) using modeFRONTIER software. The shape of each bladelet configuration was defined by the span, sweep angle, dihedral angle, twist angle and the taper ratio. The three simultaneous objectives were to maximize the coefficient of power, while minimizing the coefficients of thrust and blade twisting moment. A constraint of the Betz Limit was placed on the maximum allowable power coefficient.

A multi-dimensional response surface based on radial basis functions was created for each of the three objectives and coupled with the NSGA-II optimization algorithm to arrive at a Pareto frontier. Four virtual Pareto designs were selected at random from the Pareto frontier and validated in OpenFOAM. Out of the four selected designs, the Pareto design least sensitive to geometric defects is presented.

It was demonstrated that bladelets can increase power output of the wind turbine rotor and that the proposed multi-objective optimization framework is capable of identifying several candidate blade+bladelet configurations in multi-dimensional design space. It is expected that even higher performance of a blade+bladelet combination is possible if both blade and the bladelet shapes are optimized together and if more accurate response surfaces are used having more support points.

ACKNOWLEDGMENTS

REFERENCES

[1] N.N. Gavrilovic, B.P. Rasuo, G.S. Dulikravich and V. Parezanovic, "Commercial aircraft performance improvement by using winglets," *FME Transactions,* vol. 43, no. 1, January 2015, pp. 1-8.

[2] S.R. Reddy, H. Sobieczky, G.S. Dulikravich and A. Abdoli, "Multi-Element Winglets: Multi-Objective Optimization of Aerodynamic Shapes", *AIAA J. of Aircraft,* Vol. 5, No. 4, pp. 992-1000, 2016.

[3] A.A. Bazmi and G. Zahedi. "Sustainable Energy Systems: Role of Optimization Modeling Techniques in Power Generation and Supply—a Review", *Renewable Sustainable Energy Reviews,* Vol. 15, pp 3480–500, 2011

[4] A. Evans, V. Strezov and T.J. Evans, "Assessment of Sustainability Indicators for Renewable Energy Technologies", *Renewable Sustainable Energy Reviews,* Vol. 13, pp 1082–1088, 2009

[5] Q. Zhao, C. Sheng and A. Afjeh, "Computational Aerodynamic Analysis of Offshore Upwind Downwind Turbines," *Journal of Aerodynamics,* Vol 2014, Article ID 860637, 2014

[6] S.L. Wood and R. Deiterding, "A Lattice Boltzmann Method for Horizontal Axis Wind Turbine Simulation," *14th International Conference on Wind Engineering,* Porto Alegre, Brazil, June 21-26, 2015

[7] N. Tobin, A.M. Hamed, and L.P. Chamorro, "An Experimental Study on the Effects of Winglets on the Wake and Performance of a Model Wind Turbine," *Energies*, Vol 8, pp 11955-11972, 2015

[8]. M. Gaunaa and J. Johansen, "Determination of the Maximum Aerodynamic Efficiency of Wind Turbine Rotors with Winglets," *Journal of Physics: Conference Series*, Vol. 75, pp 1-12, 2007

[9] D. Gertz, D.A. Johnson and N. Swytink-Binnema, "An Evaluation Testbed for Wind Turbine Blade Tip Designs – Winglet Results," *Wind Engineering,* Vol. 36, pp. 389-410, 2012

[10] E. Ferrer and X. Munduate, "Wind Turbine Blade Tip Comparison Using CFD," *Journal of Physics: Conference Series*, Vol. 75, pp 1-10, 2007

[11] Vestas, Vestas V27-225 kW, 50 Hz Wind turbine with tubular/lattice tower Item no.: 941129 Version 1.2.0.24, Vestas, 1994.

[12] F. Juretic, "cfMesh User Guide," version 1.1, Creative Fields, Ltd. 2015

[13] OpenFOAM, Open Source Field Operation and Manipulation, Software Package, Ver. 2.2.0, OpenCFD Ltd., http://www.opencfd.co.uk/openfoam/, 2000.

[14] W. Zhao, P. Cheng and D. Wan, "Numerical Computation of Aerodynamic Performances of NREL Offshore 5-MW Baseline Wind Turbine," *Proceedings of the Eleventh Pacific/Asia Offshore Mechanics Symposium*, Shanghai, China, October 12-16, 2014

[15] N. Stergiannis, C. Lacor, J.V. Beeck and R. Donnelly, "CFD Modelling Approaches Against Single Wind Turbine Wake Measurements using RANS," *Journal of Physics: Conference Series*, Vol. 753, pp 1-16, 2016

[16]. F. Menter, "Two Equation Eddy-Viscosity Turbulence Models for Engieering Applications," *AIAA Journal,* Vol 32, pp 1598 – 1605, 1994

[17]. modeFRONTIER, Software Package, Ver. 4.5.4, ESTECO, Trieste, Italy, 2014

[18] T. Burton, D. Sharpe, N. Jenkins, E. Bossanyi, *Wind Energy*, John Willey & Sons Book Co., Chichester, England, 2001.

[19] M.J. Colaco and G.S. Dulikravich, "A Survey of Basic Deterministic, Heuristic and Hybrid Methods for Single-Objective Optimization and Response Surface Generation", Thermal Measurements and Inverse Techniques, (edited by Orlande, H. R. B., Fudym, O., Milet, D., and Cotta, R.), Taylor and Francis, Philadelphia, Chapter 10, pp. 355–405, May 2011

[20] I.M. Sobol, "Distribution of Points in a Cube and Approximate Evaluations of Integrals," *U.S.S.R. Computational Mathematics and Mathematical Physics,* Vol. 7, pp 86-112, 1967

[21] K. Deb, A. Pratap, S. Agarwal and T. Meyarivan, "A Fast and Elitist Multiobjective Genetic Algorithm: NSGA-II," *IEEE Transactions on Evolutionary Computation*, Vol. 6, pp 182-197, 2002